Analysis of a Bidirectional DC-DC Converter with High Voltage Gain

Behrouz Razzaghzadeh[1], Mahdi Salimi*[2]
[1]Department of Electrical Eng., Ardabil Science and Research Branch, Islamic Azad University
Ardabil, Iran
[2]Department of Electrical Eng., Ardabil Branch, Islamic Azad University, Ardabil, Iran
e-mail: m.salimi@iauardabil.ac.ir

Abstract

A novel bidirectional DC-DC converter with high conversion ratio is proposed in this paper. The proposed converter uses the three windings coupled-inductor to achieved high voltage conversion ratio. The primary side consist of a winding and secondary side consist of two windings, which these two windings are series to achieved high voltage gain.In the boost mode, a capacitor is parallel charged and series discharged by the coupled inductor. Thus, high step-up voltage gain can be achieved with an appropriate duty ratio. In the buck mode, a capacitor is series charged and parallel discharged by the coupled inductor. The bidirectional converter can have high step-down voltage gain.The stress voltage of main switches can be reduced, and efficiency can be improved. The operating principle and the steady-state analyses of the voltage gain are discussed. Finally, in 24V for low voltage, and 400V for high voltage, and 200W for output power, this converter is simulated in MATLAB.

Keywords: DC-DC Converter, tree windings, coupled inductor, high conversion ratio

1. Introduction

Because of the environmental pollution and global warming, renewable energy has become the research and the development priorities for most of the industrial countries. Bidirectional DC-DC converter can transfer the power between two dc sources. So bidirectional DC-DC converter is widely used for many green energy applications, such as wind power systems [ ], photovoltaic systems [ ], fuel cell and battery hybrid supplied power systems [ ]. Another application of bidirectional DC-DC converter is uninterruptible power supplies (UPSs) [ ]. UPSs are used for some very important loads such as computers, telecommunications and medical equipment. Batteries are commonly served as an energy storage device for the UPS system. Bidirectional DC-DC converters play an important part for back-up energy system. However, photovoltaic (PV) solar or wind power cannot provide sufficient power when the load is suddenly increased [4]-[6]. Because the renewable systems cannot provide a stable power for user, the renewable energy systems and battery can be employ for the hybrid power systems [7]. When the renewable energy systems cannot supply enough power for the load, the battery must provide this power. If the power of the renewable energy systems cannot be used completely by the load, the excess energy can be used to charge the battery [8]-[10]. Because the bidirectional DC–DC converters can transfer the power between two DC sources in either direction, these converters are widely used for renewable energy hybrid power systems, hybrid electric vehicle energy systems and uninterrupted power supplies [11]-[12]. The topologies of these converters have the isolated and non-isolated types for different applications. The isolated types include the flyback type [13]-[14], forward-flyback type [15]-[16], half-bridge type [17]-[18] and full-bridge type [19]. These converters can achieve high voltage gain by adjusting the turns ratio of the transformer. The bidirectional flyback converter has the simple structure and easy control but the switches of this converter have high voltage stresses. Thus, this converter is applied for low power applications. To reduce the voltage stresses on the switches, the energy regeneration techniques used [20]. The non-isolated types include the multi-level type, switched-capacitor type, cuk/cuk type, sepic/zeta type, buck-boost type, coupled-inductor type, three-level type and conventional buck/boost type [21]. In multi-level and switched-capacitor types, if high voltage gain needed, more switches and capacitors are required. Also, the control

circuits of these converters are complicated. For the cuk/cuk and sepic/zeta types, the efficiency are low because these converters cannot provide wide voltage conversion range [22]-[24]. Compare with [25], the proposed converter successfully developed to high conversion ratio bidirectional dc-dc converter with a three windings coupled inductors whit low duty cycle, and the switches voltage stress reduced and efficiency increase in boost and buck mode.

The proposed bidirectional converter is analysed, and its operation in boost and buck mode is described in section II. Steady-state analysis and equations of the boost and buck mode described in section III and Simulation results described in section IV.

2. Operating Principle of the Proposed Converter

Figure 1 shows the circuit configuration of the proposed converter. It is used to bidirectional transfer the energy between the DC source V_{in} in the low-voltage side and the DC source V_o in the high-voltage side.
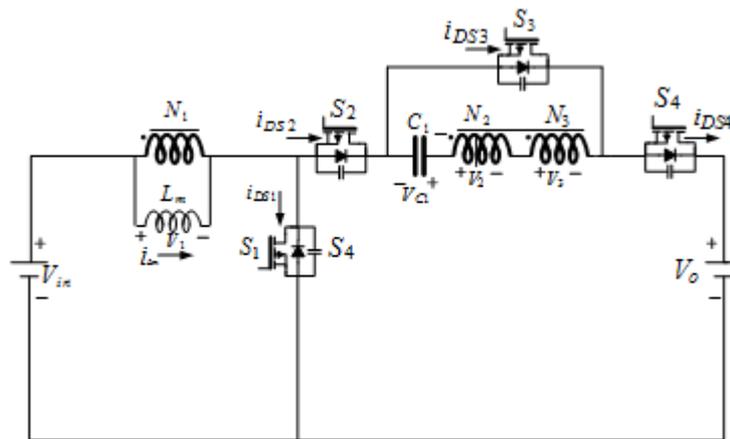
Figure 1. The proposed converter

When the proposed converter operated in the boost mode, a capacitor is parallel charged and series discharged by the coupled inductor. When the proposed converter operated in the buck mode, a capacitor is series charged and parallel discharged by the coupled inductor. In the boost mode operation, S_1, S_2 is the main switches and the buck mode, main switches are S_3, S_4 and S_7.

A. Boost-mode Operation

Figure 2(a) shows the waveforms and Figure 2(b) and 2(c) shows the current flow path of the proposed converter in boost mode. There are two operating modes in one switching period of the proposed converter. The main switch is s_1, s_2 for each mode.
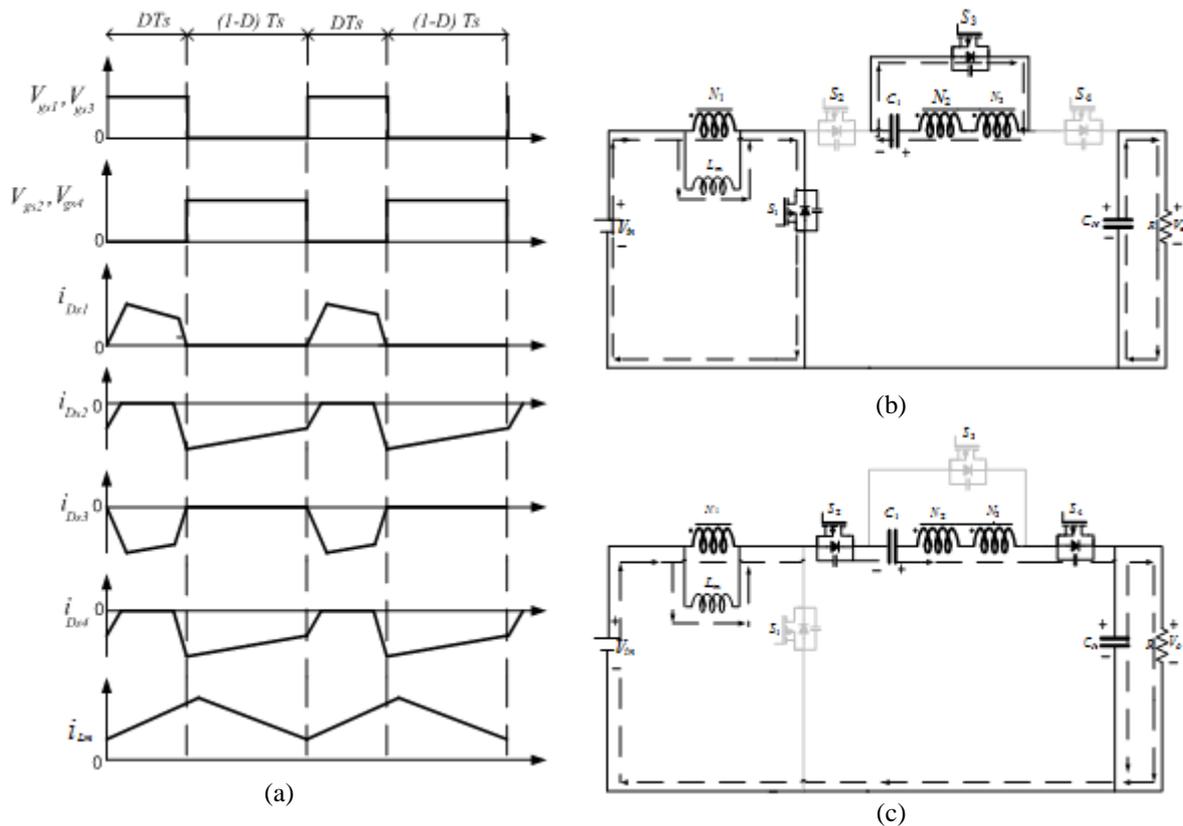
Figure 2. (a) waveforms of boost mode, (b) and (c) Current-flow path of the operating mode during one switching period in the boost mode.

The operating modes are described below:

1) Mode I $[t_0 - t_1]$: S_1, S_3 turn on and S_2, S_4 turn off in $t = t_0$. The current-flow path is shown in Figure 2(b). The dc source V_{in} charges the magnetizing inductor L_m , and the charging capacitor C_1 via the coupled inductor. Voltage V_{C1} is equal to $2nV_{in}$ and a capacitor is charged in parallel. The output capacitor C_H provides energy to load R. This operating mode ends when switch S_1 is turned off at $t = t_1$.

2) Mode II $[t_1 - t_2]$: S_2, S_4 turn on and S_1, S_3 turn off. The current flow path is shown in Figure 2(c). The coupled inductor, dc source V_{in}, and capacitor C_1 are connected in series to charge the output capacitor C_H and load R. This operating mode ends when switch S_2, S_4 is turned off at $t = t_2$ and beginning of the next switching period.

B. Buck-mode Operation

Figure 3(a) shows the waveforms and Figure 3(b) and 3(c) shows the current flow path of the proposed converter in boost mode. There are two operating modes in one switching period of the proposed converter. The main switch is s_4 for each mode.
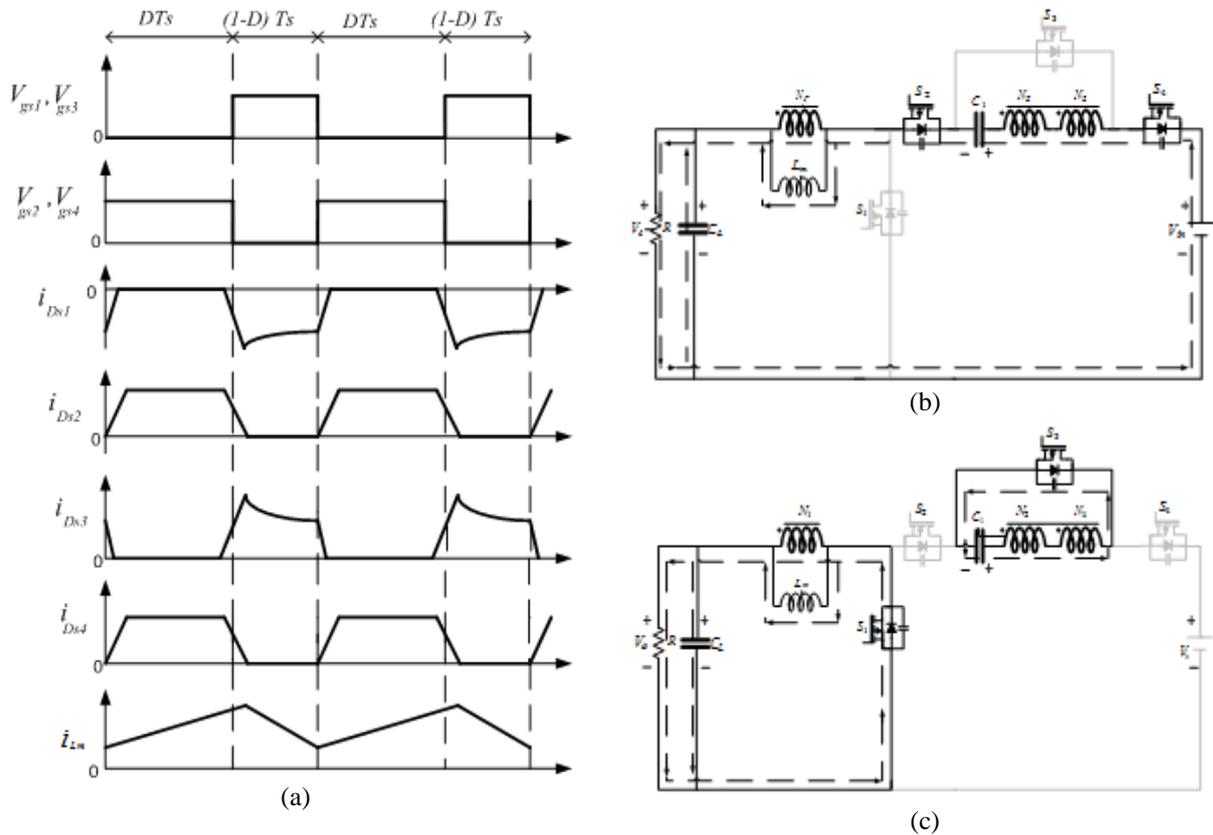
Figure 3. (a) waveforms of buck mode, (b) and (c) Current-flow path of the operating mode during one switching period in the buck mode

The operating modes are described below:

1) Mode I [$t_0 - t_1$]:S_2, S_4 turn on and S_1, S_3 turn off. The current flow path is shown in Figure 3(b). Capacitor C_1 and the secondary side coil N_2, N_3 are still charged in series by V_{in}, and the magnetizing inductor L_m is also charged. The output capacitor C_L provide the energy to load R. This operating mode ends when switch S_2, S_4 is turned off at $t = t_1$.

2) Mode II [$t_1 - t_2$]: S_1, S_3 turn on and S_2, S_4 turn off at $t = t_1$. The current flow path is shown in Figure 3(c). The energy of capacitor C_1 discharges to the output capacitor C_L and load R through the coupled inductors. The magnetizing inductor L_m also discharges to the output. This operating mode ends when switch S_1 is turned off at $t = t_2$.

3. Steady-state analysis of the proposed converter

After the mode analysis of the boost and buck mode operations, the following equations and voltage gain in the steady state of the proposed converter can be derived. The equations of the turn ratio of the coupled inductor are defined as

$$n = \frac{N_2}{N_1} = \frac{N_3}{N_1} \tag{1}$$

A. Boost-mode Operation

There are two operating modes in one switching period of the proposed converter. In the time period of mode I, the following equations can be written based on Figure 2(b). The voltage on the primary and secondary sides of the coupled inductors are showed as

$$V_1^I = V_{in} \tag{2}$$

$$V_2^I = V_3^I = nV_1^I = nV_{in} \tag{3}$$

Also the voltage of capacitor C_1 can be written as follows:

$$V_{c1} = V_2^I + V_3^I = 2nV_1^I = 2nV_{in} \tag{4}$$

Based on Figure 2(c), in modes II, the voltage on the secondary side of the coupled inductor can be formulated as follows:

$$V_2^{II} + V_3^{II} = V_{in} - V_1^{II} + V_{c1} - V_o \tag{5}$$

$$2nV_1^{II} = V_{in} - V_1^{II} + 2nV_{in} - V_o \tag{6}$$

$$V_1^{II} = \frac{(1 + 2n)V_{in} - V_o}{1 + 2n} \tag{7}$$

Using the volt-second balance principle on the magnetizing inductor L_m, the following is given:

$$\int_0^{DT_s} V_1^I \, dt + \int_{DT_s}^{T_s} V_2^{II} \, dt = 0 \tag{8}$$

Also, the voltage stress of the main switch S_1 can be expressed as

$$V_1^{II} = V_{in} - V_{s1} \tag{9}$$

Substituting (2) and (9) into (8), voltage stress is obtained as

$$V_{DS1} = \frac{V_{in}}{1 - D} \tag{10}$$

Substituting (2) and (7) into (8), the voltage gain of the boost state operation is obtained as

$$M_{boost} = \frac{V_H}{V_L} = \frac{1 + 2n}{1 - D} \tag{11}$$

B. Buck-mode Operation

In the time period of mode I, the following equations can be written based on Figure 3(b). The voltage on the primary and secondary sides of the dual coupled inductors are showed as

$$V_2^I + V_3^I = V_{in} - V_1^I + V_{c1} - V_o \tag{12}$$

$$2nV_1^I = V_{in} - V_1^I + 2nV_L - V_o \tag{13}$$

$$V_1^I = \frac{(1 + 2n)V_L - V_H}{1 + 2n} \tag{14}$$

The voltage on the primary and secondary sides of the coupled inductor in mode II can be written based on Figure 3(c):

$$V_1^{II} = V_{in} \tag{15}$$

$$V_2^{II} = V_3^{II} = nV_1^{II} = nV_{in} \tag{16}$$

Thus, the voltage of capacitor $C1$ is also derived on Figure 3(c). The voltage is expressed as

$$V_{c1} = V_2^I + V_3^I = 2nV_1^I = 2nV_{in} \tag{17}$$

Using the volt second balance principle on the magnetizing inductor L_m, the following is given:

$$\int_0^{DT_s} V_1^I \, dt + \int_{DT_s}^{T_s} V_1^{II} \, dt = 0 \tag{18}$$

Substituting (12) and (13) into (16), the voltage gain of the buck-mode operation is obtained as

$$M_{buck} = \frac{V_{in}}{V_o} = \frac{D}{1 + 2n} \tag{19}$$

4. Simulation Results

To illustrate the performance and the functions of the proposed converter, this converter is implemented in the MATLAB. The specifications are:
1) dc voltage V_L is 24 V and V_H is 400 V;
2) output power: 200 W;
3) switching frequency: 50 kHz;
4) Coupled inductor: $N_1 : N_2 : N_2 = 1 : 5 : 5$, $L_m = 100$ μH;
5) Capacitors C_1 and C_2 is 15μF;
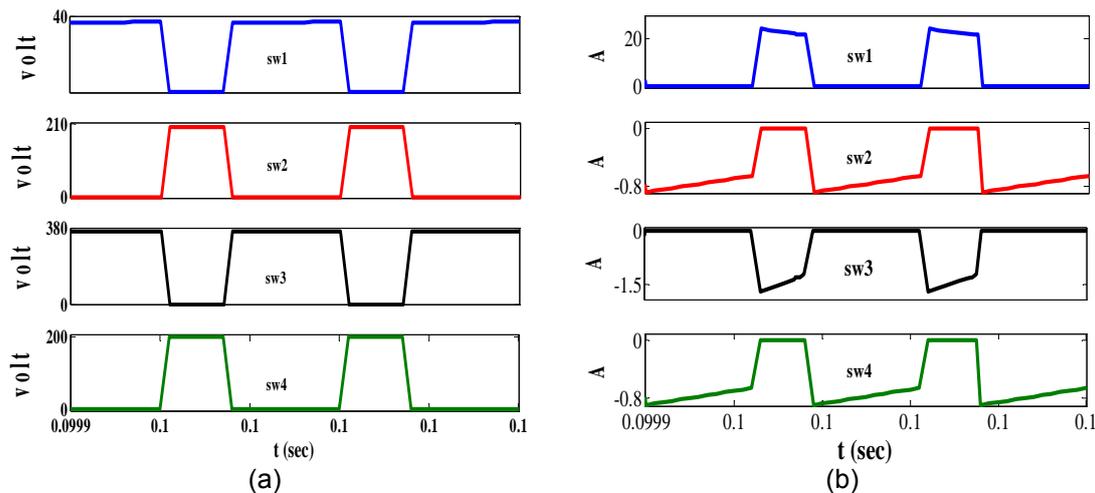
Figure 4. Simulation results in the boost mode under full load P_o = 200 W. (a) voltage stress of switches, (b) current of switches

In Figure (4), the waveforms are the boost mode operation at full load P_o = 200 W, $V_{in} = 24$ V, and $V_{out} = 400$ V. The waveform shows that the steady-state analysis of the boost mode is correct. According to (11) and specifications, the duty cycle is 34.5%. Figure 4(a) shows waveform of voltage stress of switches. According to (10) stress voltage of main switches S_1 equal in 36.65 V. Because the proposed converter works in the boost mode, stress voltage in low side switch S_1 reduced. Figure 4(b) shows waveform of current of switches. Because the proposed converter works in the boost mode, stress voltage in low side switches S_1 reduced.
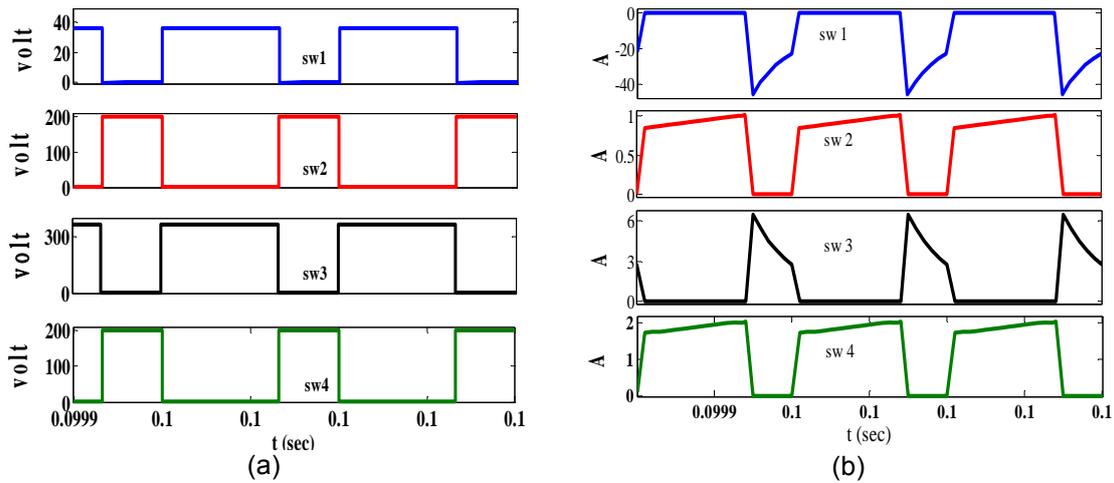
Figure 5. Simulation results in the buck mode under full load Po = 200 W. (a) voltage stress of switches, (b) current of switches

In Figure (5), the waveforms are the buck mode operation at full load Po = 200 W, V_{in} = 400 V, and V_{out} = 24 V. According to (19) and specifications, the duty cycle is 65.5%. Figure 5(a) shows waveform of voltage stress of switches. Stress voltage of main switch S_7 is 165 V. Figure 5(b) shows waveform of current of switches. Because the proposed converter works in the buck mode, stress voltage in high side switch S_4 reduced.

Also, According the equation (20) curve of efficiency in buck and boost mode are given as figure 6.

$$efficiency = \frac{P_{out}}{P_{in}} = \frac{V_o I_o}{V_{in} I_{in}} \tag{20}$$
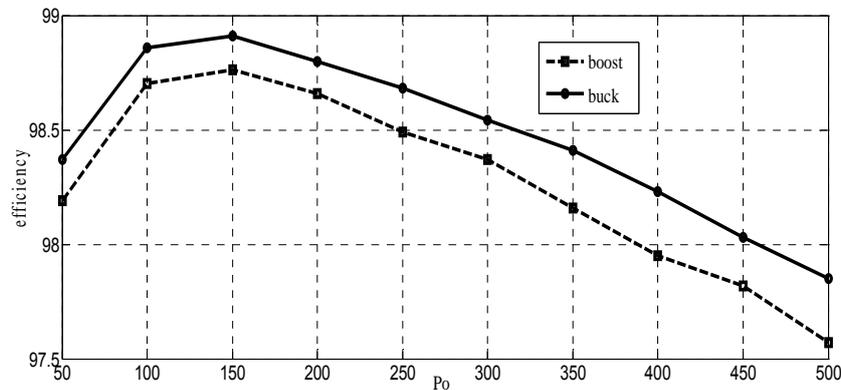
Figure 6. Efficiency in the boost and buck mode

Figure (6) shows the measured efficiency of proposed converter in boost and buck mode at V_L = 24 V and V_H = 400 V. the maximum efficiency in the boost mode is 98.76% at P_o = 150 W and full load efficiency is 98.66% at P_o = 200 W. The maximum efficiency in the buck mode is 98.91% at P_o = 150 W and full load efficiency is 98.8% at P_o = 200 W.
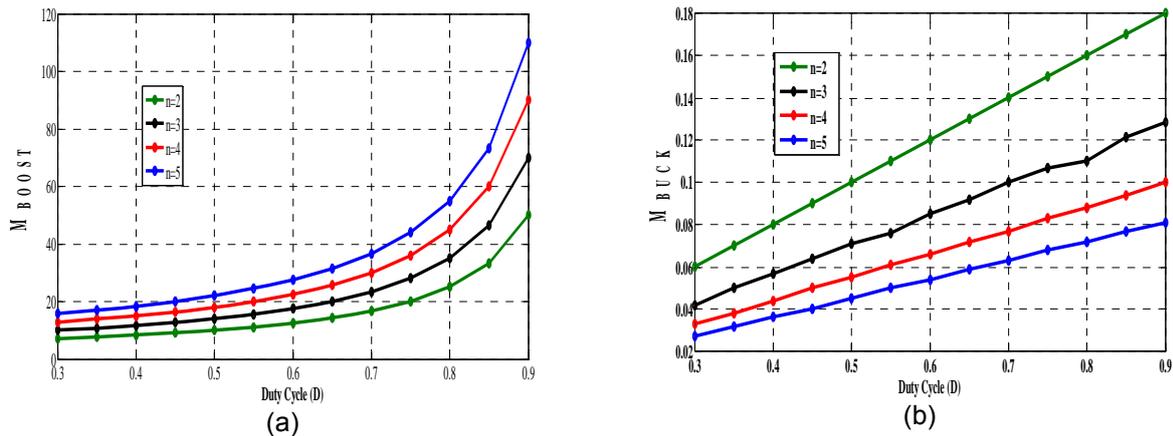
Figure 7. voltage gain curves under different turn ratio, (a) boost mode, (b) buck mode

Figure 7(a) shows the voltage gain versus the duty cycle under various turns ratio of coupled inductors in the boost mode.in the boost mode, if the turn ratio increases, voltage gain will also be increased

Figure 7(b) shows the voltage gain versus the duty cycle under various turns ratio of coupled inductors in the buck mode.in the buck mode, if the turn ratio increases, voltage gain will be decreases.

5. Conclusion

This paper has proposed a high-efficiency, and high step-up and step-down bidirectional dc–dc converter. This converter successfully developed a high-voltage gain bidirectional dc-dc converter by using three winding coupled inductor. By using the a capacitor charged in parallel and discharged in series by the coupled inductor, high conversion ratio and high efficiency has been achieved. The voltage gain increased by using a coupled inductor with a low turn ratio. Simulation results shows that the efficiency at full load $P_o = 200\,W$ is 98.66% in the boost mode and 98.8% in the buck mode.

References

[1] C Cecati, F Ciancetta, and P Siano. "A multilevel inverter for photovoltaic systems with fuzzy logic control". *IEEE Trans. Ind. Electron*. 2010; 57(12): 4115–4125.
[2] Ghadimi, Noradin. "Using HBMO Algorithm to Optimal Sizing & Sitting of Distributed Generation in Power System". *Bulletin of Electrical Engineering and Informatics*. 2014; 3(1).
[3] R Seyezhai, HarineeHarinee, Nagarajan Nagarajan. "Simulation and Implementation of Soft-Switched Interleaved DC-DC Boost Converter for Fuel Cell Systems". *BEEI*. 2012; 1(3).
[4] JY Lee and SN Hwang. "Non-isolated high-gain boost converter using voltage-stacking cell". *Electron. Lett*. 2008; 44(10): 644–645.
[5] R Seyezhai, R Anitha, S Mahalakshmi, M Bhavani. "High Gain Interleaved Boost Converter for Fuel Cell Applications". *BEEI*. 2013; 2(4).
[6] Luiz Henrique SC Barreto, Paulo Peixoto Praca, Demercil S Oliveira Jr. and Ranoyca NAL Silva. "High-voltage gain boost converter based on three-state commutation cell for battery charging using PV panels in a single conversion stage". *IEEE Trans. Power Electron*. 2014; 29(1): 150–158.
[7] Nagulapati Kiran. "Sliding Mode Control of Buck Converter". BEEI. 2014; 3(1).
[8] R Gules, JDP Pacheco, HL Hey and J Imhoff. "A maximum power point tracking system with parallel connection for PV stand-alone applications". *IEEE Trans. Ind. Electron*. 2008; 55(7): 2674–2683.
[9] Ghadimi N. An adaptive neuro-fuzzy inference system for islanding detection in wind turbine as distributed generation. Complexity. doi: 10.1002/cplx.21537. 2014.
[10] RY Duan and JD Lee. "High-efficiency bidirectional dc–dc converter with coupled inductor". *IET Power Electron*. 2012; 5(1): 115–123.
[11] H Tao, JL Duarte, and MAM Hendrix. "Line-interactive UPS using a fuel cell as the primary source". *IEEE Trans. Ind. Electron*. 2008; 55(8): 3012–3021.

[12] YP Hsieh, JF Chen, TJ Liang, LS Yang. "Novel high step-up DC-DC converter for distributed generation system". *IEEE Trans. Ind. Electron.* 2013; 60(4): 1473-1482.
[13] Venkatesan K. "*Current mode controlled bidirectional flyback converter*". Proc. IEEE PESC. 1989: 835–842.
[14] Chen G, Lee YS, Hui SYR, Xu D, Wang Y. "Actively clamped bidirectional flyback converter". *IEEE Trans. Ind. Electron.* 2000; 47(4): 770–779.
[15] Huber L, Jovanovic MM. "Forward-flyback converter with current-doubler rectifier: analysis, design, and evaluation results". *IEEE Trans. Power Electron.* 1999; 14(1): 184–192.
[16] Zhang F, Yan Y. "Novel forward–flyback hybrid bidirectional DC–DC converter". *IEEE Trans. Ind. Electron.* 2009; 56(5): 1578–1584.
[17] Li H, Peng FZ, Lawler JS. "A natural ZVS medium-power bidirectional DC–DC converter with minimum number of devices". *IEEE Trans. Ind. Appl.* 2003; 39(2): 525–535.
[18] Peng FZ, Li H, Su GJ, Lawler JS. "A new ZVS bidirectional DC–DC converter for fuel cell and battery Application". *IEEE Trans. Power Electron.* 2004; 19(1): 54–65.
[19] Lin BR, Huang CL, Lee YE. "Asymmetrical pulse-width modulation bidirectional DC–DC converter". *IET Power Electron.* 2008; 1(3): 336–347.
[20] Mi C, Bai H, Wang C, Gargies S. "Operation, design and control of dual H-bridge-based isolated bidirectional DC–DC converter". *IET Power Electron.* 2008; 1(4): 507–517.
[21] Khan FH, Tolbert LM, Webb WE. "Hybrid electric vehicle power management solutions based on isolated and nonisolated configurations of multilevel modular capacitor-clamped converter". *IEEE Trans. Ind. Electron.* 2009; 56(8): 3079–3095.
[22] Monge SB, Alepuz S, Bordonau J. "A bidirectional multilevel boost–buck DC–DC converter". *IEEE Trans. Power Electron.* 2011; 26(8): 2172–2183.
[23] Peng FZ, Zhang F, Qian Z. "A magnetic-less DC–DC converter for dual-voltage automotive systems". *IEEE Trans. Ind. Appl.* 2003; 39(2): 511–518.
[24] Lee YS, Chiu YY. "Zero-current-switching switched-capacitor bidirectional DC–DC converter", *IEE Proc. Inst. Elect. Eng. Electr. Power Appl.* 2005; 152(6): 1525–1530.
[25] Ko YP, Lee YS, Chao WH. "Analysis, design and implementation of fuzzy logic controlled quasi-resonant zero-current switching switched-capacitor bidirectional converter". *IET Power Electron.* 2011; 4(6): 683–692.
[26] X Hu, Ch Gong. "A High Gain Input-Parallel Output-Series DC/DC Converter with Dual Coupled-Inductors". *IEEE Trans, Ind, Electron.* 2014; 50(1).